



HAL
open science

Tritiated stainless steel (nano)particle release following a nuclear dismantling incident scenario: Significant exposure of freshwater ecosystem benthic zone

Danielle Slomberg, Mélanie Auffan, Mickaël Payet, Andrea Carboni, Amazigh Ouaksel, Lenka Brousset, Christian Grisolia, Alain Thiéry, Bernard Angeletti, Jérôme Rose

► To cite this version:

Danielle Slomberg, Mélanie Auffan, Mickaël Payet, Andrea Carboni, Amazigh Ouaksel, et al.. Tritiated stainless steel (nano)particle release following a nuclear dismantling incident scenario: Significant exposure of freshwater ecosystem benthic zone. *Journal of Hazardous Materials*, 2024, 465, pp.133093. 10.1016/j.jhazmat.2023.133093 . hal-04447287

HAL Id: hal-04447287

<https://hal.science/hal-04447287v1>

Submitted on 25 Oct 2024

HAL is a multi-disciplinary open access archive for the deposit and dissemination of scientific research documents, whether they are published or not. The documents may come from teaching and research institutions in France or abroad, or from public or private research centers.

L'archive ouverte pluridisciplinaire **HAL**, est destinée au dépôt et à la diffusion de documents scientifiques de niveau recherche, publiés ou non, émanant des établissements d'enseignement et de recherche français ou étrangers, des laboratoires publics ou privés.

Tritiated stainless steel (nano)particle release following a nuclear dismantling incident scenario: significant exposure of freshwater ecosystem benthic zone

Danielle L. Slomberg^{1*}, Mélanie Auffan^{1,2}, Mickaël Payet³, Andrea Carboni¹, Amazigh Ouaksel¹, Lenka Brousset⁴, Bernard Angeletti¹, Christian Grisolia³, Alain Thiéry⁴, Jérôme Rose^{1,2}

¹CNRS, Aix-Marseille Univ., IRD, INRAE, CEREGE, 13545 Aix-en-Provence, France

²Civil and Environmental Engineering Department, Duke University, Durham, North Carolina 27707, United States

³CEA, IRFM, F-13108, Saint Paul lez Durance, France

⁴CNRS, IRD, IMBE, Aix-Marseille Univ, Avignon Univ., Marseille, France

*Corresponding author: slomberg@cerege.fr

Keywords: stainless steel particles, tritium, nuclear reactor dismantling, aquatic mesocosm, environmental exposure, ecotoxicity, radiotoxicity, sediment accumulation

Abstract

Nuclear facilities continue to be developed to help meet global energy demands while reducing fossil fuel use. However, an incident during the dismantling of these facilities could accidentally release tritiated particles (e.g., stainless steel) into the environment. Herein, we investigated the environmental dosimetry, fate, and impact of tritiated stainless steel (nano)particles (1 mg.L⁻¹ particles and 1 MBq.L⁻¹ tritium) using indoor freshwater aquatic mesocosms to mimic a pond ecosystem. The tritium (bio)distribution and particle fate and (bio)transformation were monitored in the different environmental compartments over 4 weeks using beta counting and chemical analysis. Impacts on picoplanktonic and picobenthic communities, and the benthic freshwater snail, *Anisus vortex*, were assessed as indicators of environmental health. Following contamination, some tritium (~16%) desorbed into the water column while the particles rapidly settled onto the sediment. After 4 weeks, the particles and the majority of the tritium (>80%) had accumulated in the sediment, indicating a high exposure of the benthic ecological niche. Indeed, the benthic grazers presented significant behavioral changes despite low steel uptake (<0.01 %). These results provide knowledge on the potential environmental impacts of incidental tritiated (nano)particles, which will allow for improved hazard and risk management.

Environmental Implication

Tritiated stainless steel (nano)particles may accidentally be released into freshwater environments during a nuclear facility dismantling incident. These particles, containing radioactive tritium and potentially toxic metals, represent a hazardous material of emerging concern. To date, little is known about the behavior, fate and toxicity of such tritiated particles and it is therefore difficult to anticipate their environmental impacts. The current work helps address this by providing the first elements of knowledge on the dosimetry and particle fate in different environmental compartments, as well as identifying the organisms and ecological niches likely to be exposed, using an environmentally relevant exposure scenario.

45 1 Introduction

46
47 Natural nanoparticles or colloids (from natural mineral weathering, ocean spray, volcanoes, etc.)
48 have been known to be involved in the transport of pollutants in surface and groundwaters for
49 decades. Indeed, in 1989, McCarthy and Zachara first called attention to “the potentially critical, but
50 poorly understood role of colloids in facilitating contaminant transport,” with a particular emphasis
51 on the transport of radionuclides.¹ Since then, a large number of studies have focused on the
52 mechanisms, thermodynamics, and kinetics of the bio-physico-chemical interactions between these
53 natural nanoparticles and a variety of pollutants (e.g. metals, metalloids, radionuclides, organics).²⁻⁵

54 In recent years, another source of nanoparticles in the environment has been identified, resulting from
55 the release of incidental, anthropogenic nanoparticles formed due to processes such as combustion,
56 wear, corrosion, and abrasion over the course of a material’s lifecycle.⁶ In the case of nuclear energy
57 facilities, incidental nanoparticles can be produced during routine reactor operation and maintenance
58 (e.g. tungsten nanoparticles),^{7,8} and decommissioning phases (e.g. stainless steel and cement).⁹ Under
59 normal operating and decommissioning conditions, these particles are contained due to the use of
60 ventilation systems equipped with High Efficiency Particulate Air (HEPA) filters.¹⁰ However, in the
61 case of a containment system failure, such incidental nanoparticles could be subsequently released
62 into the environment and their environmental behavior, fate, hazard, and role in vectorizing
63 radioactive contaminants such as tritium still requires investigation.¹¹

64 Tritium (³H), present in nuclear reactors as a by-product or reaction source, is a highly mobile,
65 radioactive isotope of hydrogen (half-life of 12.3 years) and has already been shown to be radiotoxic
66 in the environment.¹²⁻¹⁵ Tritium easily exchanges with water to form tritiated water, and can also
67 bind to carbon chains of organic molecules.^{14,16-18} The organic complexation of tritium is known to
68 enhance its bioaccumulation in the environment and favor its trophic transfer.¹⁹ Tritium can also be
69 adsorbed at the surface of natural nanoparticles where it substitutes the protons of the structural
70 hydroxyls.²⁰ As previously mentioned, radionuclide adsorption onto natural nanoparticles is a well-
71 known mechanism controlling their transport and migration in surface and groundwaters.^{21,22}
72 However, many gaps remain in understanding how tritium association with or transport by incidental,
73 anthropogenic nanoparticles generated during dismantling activities will impact its environmental
74 behavior and fate.⁹

75 As such, tritiated stainless steel (nano)particles, which may be incidentally emitted into freshwater
76 environments during decommissioning activities, were selected as the focus for this study. Once
77 released into aquatic ecosystems, these particles may release constituting metals (e.g. Cr, Ni, Mo, Fe)
78 and tritium into the water column. They may also agglomerate and settle down due to their density
79 (i.e. 7900 kg.m⁻³) and an isoelectric point at the environmentally relevant pH of 7.8.^{23,24} To date, little
80 is known about the behavior, fate and toxicity of such incidental tritiated stainless steel
81 (nano)particles and it is therefore difficult to anticipate the effects of an accidental release. Previous
82 studies have assessed the ecotoxicity of metallic and metal oxide-based nanoparticles (e.g. Ag, Au,
83 CuO, ZnO, CeO₂) towards aquatic invertebrates (e.g. bivalves, gastropods, crustaceans) and
84 demonstrated that these nanoparticles can increase reactive oxygen species (ROS) production and
85 lead to toxicity.^{25,26} The possibility for nanoparticles to cross biological barriers and accumulate in
86 aquatic organisms has also been linked to toxicity (Auffan et al 2011).²⁷ Based on this knowledge,
87 any stainless steel (nano)particle toxicity will likely be related to particle solubility and/or the ability
88 to bioaccumulate in organisms. Vernon et al.²⁸ reported a lack of genotoxicity and low accumulation
89 in the marine filter feeders *Mytilus galloprovincialis* exposed to 1 mg.L⁻¹ stainless steel
90 (nano)particles (non-radioactive) under controlled conditions. However, there have been no prior
91 studies on the impacts of stainless steel (nano)particles to freshwater organisms. In addition, further

92 work employing radioactive tritiated stainless steel (nano)particles has yet to be completed to
93 elucidate the potential combined impacts.

94 Depending on the physico-chemical properties and transformations of the tritiated stainless steel
95 (nano)particles in natural environments, the organisms and ecological niches likely to be exposed
96 will differ (e.g. benthic *versus* planktonic compartments, filter-feeders *versus* benthic grazers,
97 primary producers *versus* consumers). Moreover, the presence of dissolved ions and natural
98 suspended matter in natural environments must be taken into account, as they will strongly modify
99 tritiated stainless steel (nano)particle behavior and fate.²⁹⁻³¹ To date, the main limitation for a better
100 assessment of the behavior of tritium associated to or transported by incidental nanoparticles (e.g.
101 stainless steel) is the difficulty in monitoring their behavior and fate in complex and relevant
102 environmental matrices (e.g. sediment, biota). Due to their nanometric size and heterogeneous
103 distribution, it remains challenging to link macroscopic effects (e.g. ecotoxicity, distribution within
104 organisms) to the evolution of the particle's nanometric properties (e.g. surface
105 adsorption/desorption, homo/hetero-aggregation) in a relevant exposure scenario.³² To this end,
106 aquatic mesocosms are an invaluable experimental tool due to their ability to mimic realistic
107 contamination scenarios (e.g. low doses) that account for the complexity and synergies between
108 contaminants and natural components, while allowing for the monitoring of multiple endpoints and
109 the investigation of the impacts on several ecological niches.^{33,34}

110 Herein, we investigated the environmental dosimetry, fate, and impact of tritiated stainless steel
111 (nano)particles on a pond ecosystem under static conditions using indoor freshwater aquatic
112 mesocosms designed to simulate a one-time contamination following a dismantling incident scenario.
113 The contamination was performed by injecting tritiated stainless steel particles (or hydrogenated
114 stainless steel particles as a non-radioactive control) into the mesocosm for a final concentration of 1
115 mg.L⁻¹ incidental (nano)particles and 1 MBq.L⁻¹ tritium. The tritium (bio)distribution and stainless
116 steel particle fate and (bio)transformation were monitored in the different environmental
117 compartments (e.g., water, sediment, biota) over 4 weeks, using beta counting and chemical analysis,
118 respectively. Impacts on picoplanktonic and picobenthic communities, as well as the benthic grazer
119 gastropod, *Anisus vortex*, were assessed as indicators of environmental health. Through these
120 investigations, our goal was to provide some of the first key knowledge on the environmental impacts
121 of radiocontaminants associated to or transported by incidental (nano)particles from the nuclear
122 energy sector, which will be crucial for improving hazard and risk management.

123 2 Materials and Methods

124 2.1 Aquatic mesocosm set-up

125 For each experiment (i.e., radioactive and non-radioactive), four indoor aquatic mesocosms (glass
126 tanks of 350 × 200 × 400 mm) were set up to mimic a natural pond ecosystem. The organisms
127 selected for this study were picoplankton and picobenthos primary producers (e.g., bacteria, algae,
128 protozoa from natural inoculum) and the benthic grazing snail, *Anisus vortex* (L., 1758), sampled
129 from a non-contaminated pond in the South of France (N 43°20'47.04", E 6°15'34.786"). The pond
130 physical-chemical parameters on the field sampling day were: electrical conductivity = 432 μS.cm⁻¹,
131 temperature = 11°C, pH = 8.1, dissolved O₂ = 8.6 mg.L⁻¹ (94% of saturation), and total dry residue
132 (organic and mineral) = 280 mg.L⁻¹.

133 Each mesocosm consisted of a bottom layer of ~2.3 kg artificial sediment (89% SiO₂, 10% kaolinite,
134 and 1% CaCO₃) covered by 150 g of water-saturated natural sediment containing primary producers
135 (sieved at 250 μm), followed by 16 L of Volvic® water, which has pH and conductivity values close
136 to those of the natural pond water. Picoplankton recovered from the natural pond surface water were

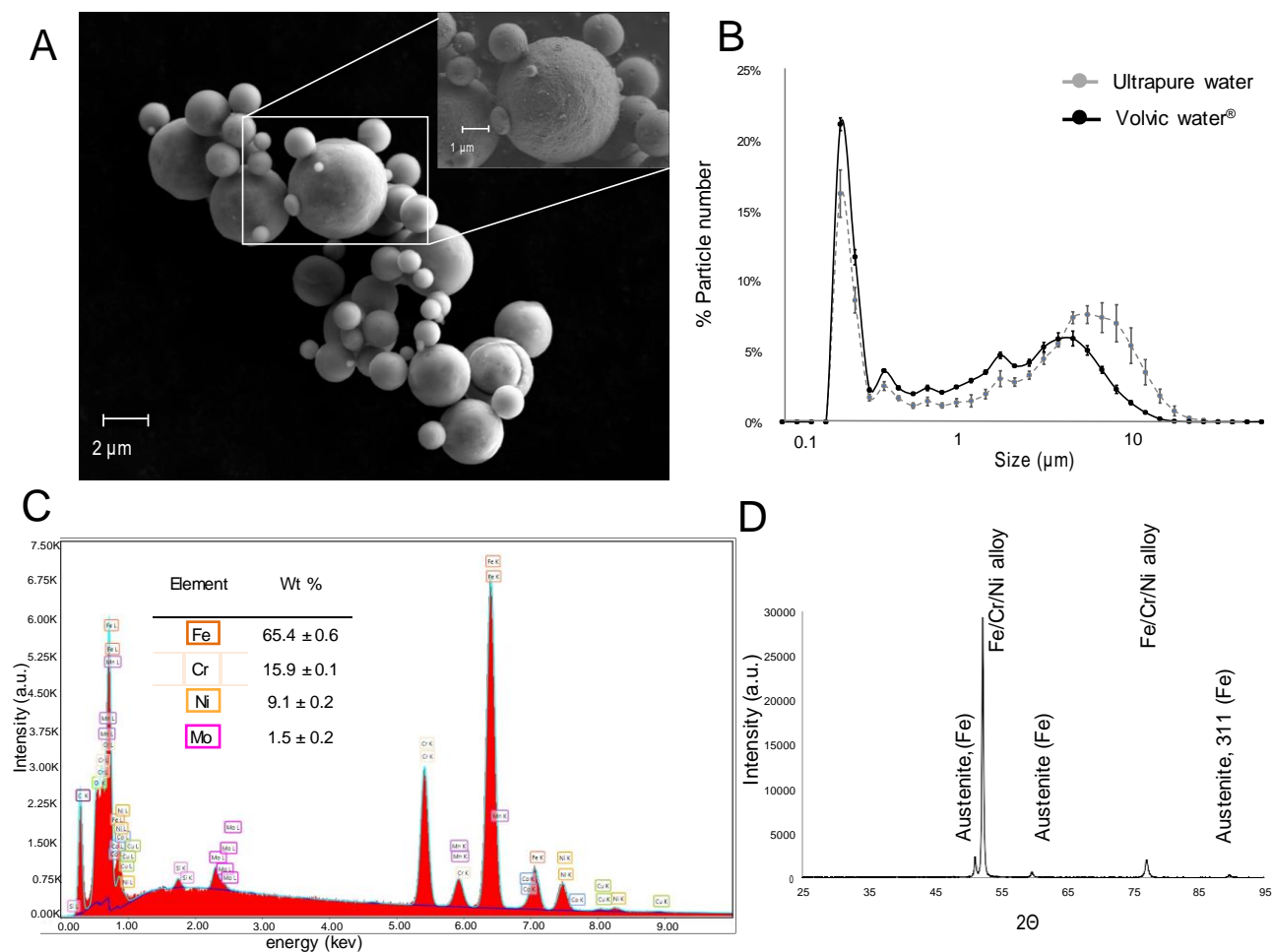
137 also added to the mesocosm. Briefly, 100 mL of pond water was sieved (250 μm), then successively
138 filtered at 2 μm and 0.2 μm . The 0.2 μm filter was then recovered and agitated in 100 mL Volvic[®]
139 water to resuspend the picoplankton, and 40 mL of this water inoculum was injected into each
140 mesocosm. A day/night cycle of 6 h/18 h was applied using full spectrum light (Viva[®] light T8 tubes
141 18 W), and the room temperature ranged between 16.0 ± 1.5 °C. The mesocosm experiments were
142 performed under static conditions, with no pumping or water circulation. Ultrapure water was added
143 to the mesocosms weekly to compensate for evaporation. Two weeks of equilibration were necessary
144 for the stabilization of the mesocosm physico-chemical parameters and the development of the
145 primary producers. Then, ~20 adult *A. vortex* (6.0 ± 0.6 mm diameter) were introduced per
146 mesocosm and acclimatized for 3 days prior to starting the experiment. More information on the
147 experimental procedure can be found in Auffan et al.³⁵

148 2.2 Tritiated and hydrogenated stainless steel particles

149 Commercial stainless steel (SS316L, Product No. FF216030) particles with a main elemental
150 composition of 69% w/w Fe, 17% w/w Cr, 10% w/w Ni, 2% w/w Mo, 1.4% w/w Mn, were purchased
151 from Goodfellow[®] (Huntingdon, England). These commercial stainless steel particles were selected
152 based on parameters defined from preliminary work in which particles were produced a stainless
153 steel rod by saw cutting.³⁶ The process used to label the stainless steel particles is based on thermally
154 activated diffusion. Tritiated stainless steel (nano)particles (T-SS) were obtained using a three-step
155 procedure developed at CEA Saclay (French Alternative Energies and Atomic Energy Commission):
156 i) the commercial SS316L particles were first treated two times at 450 °C for 2h under high pressure
157 (1.2×10^5 and 1.4×10^5 Pa, respectively) with ¹H₂ in order to stabilize the surface of the particles in a
158 reducing atmosphere; ii) during the second treatment the particles were exposed to tritium gas (³H₂)
159 at 450 °C and 1×10^5 Pa; and iii) to complete the process, a degassing step was performed to
160 eliminate any mobile tritium, which resulted in a T-SS particle specific radioactivity of 1 MBq.mg⁻¹.
161 ³⁷ This specific activity is proportional to the content of tritium trapped in the material (bound or
162 unbound). The stability of the T-SS particles with respect to the tritium content was confirmed by
163 measuring the specific activity before and after 3 months of storage in a glovebox in air. A batch
164 experiment was also conducted to determine the short-term tritium release kinetics in abiotic
165 mesocosm water (i.e., Volvic[®]) using the same T-SS particle concentration to be introduced in the
166 mesocosms (i.e., 1 mg.L⁻¹). Briefly, a 1 mg.L⁻¹ suspension of T-SS (10 mL) was prepared in Volvic[®]
167 water and stirred continuously. This suspension was sampled (2mL) at 1, 3, 6, 48, and 92 h. Each
168 aliquot was immediately filtered by centrifugation (4000xg for 1 h) using Amicon[®] Ultra-4 3 K
169 centrifugal filter devices (3 000MWCO, size retention limit ~ 1 nm, Merck-Millipore[®]) and the
170 filtrate (i.e., dissolved fraction) was measured directly by liquid scintillation counting (Tri-Carb
171 2910TR analyzer, Perkin Elmer). The % tritium (³H) release was determined using the ratio of the
172 volumetric release activity to the initial volumetric activity.

173 Surrogate, hydrogenated stainless steel (nano)particles (H-SS) were also prepared as a non-
174 radioactive control and were obtained by exposing the commercial particles to the same temperature
175 and pressure conditions, but using ¹H₂ instead of ³H₂ for the second step at 450 °C and 1×10^5 Pa.
176 The H-SS particles were characterized for size, morphology, elemental composition, and crystalline
177 phases using scanning electron microscopy (SEM) with Energy Dispersive Spectroscopy (EDS)
178 analysis, optical particle counting, and X-ray diffraction (XRD), as detailed in Experimental S1 and
179 as shown in Figure 1. Of note, the treatment process used to obtain the H-SS particles did not result
180 in any significant change in size, morphology, or elemental composition. The average SEM size for
181 the pristine commercial particles was 1.72 ± 1.14 μm , with 2 particle populations centered around
182 ~0.7 μm and ~4 μm , while for the H-SS particles the average SEM size was 1.73 ± 0.99 μm with 2
183 particle populations centered around ~0.8 μm and ~3 μm (Figure S1). Furthermore, these SEM size

184 distributions were coherent with that obtained via optical particle counting in ultrapure and Volvic®
185 water (Figure 1).
186



187
188 **Figure 1.** Hydrogenated SS particles characterization: A) SEM image (EHT = 15 kV, WD = 12.5
189 mm, BSD4A, Mag. = 3.39 kX), B) optical counter size distribution analysis in ultrapure and Volvic®
190 water (0.5 g.L⁻¹), C) Elemental composition based on EDS analysis, and D) XRD diffractogram (λ_{Co}
191 = 1.79 Å).

192 2.3 Particle exposure scenario of a lentic ecosystem

193 The aquatic mesocosm experiments were designed to simulate a one-time contamination of a pond
194 ecosystem under static conditions with tritiated steel particles (Figure 2). Stainless steel fate and
195 behavior in the mesocosms was monitored at the CEREGE using the surrogate H-SS particles, while
196 tritium distribution in the different environmental compartments was determined using T-SS particles
197 in a parallel experiment conducted at the Saclay tritium lab (CEA). The one-time contamination was
198 performed by injecting 16 mL of a suspension (in ultrapure water) containing 16 mg of H-SS or T-SS
199 for a final concentration of 1 mg.L⁻¹ stainless steel particles in the mesocosm water column. In the
200 case of the T-SS exposure, the injection of 1 mg.L⁻¹ T-SS corresponded to a tritium concentration of
201 1 MBq.L⁻¹ i.e., 1 MBq per mg of SS. Of note, due to the need to limit the production and
202 management of tritiated waste, the aquatic mesocosms exposed to T-SS particles were used to obtain
203 tritium concentrations in the different environmental compartments (i.e. sediment, biota, water
204 column), as well as a qualitative assessment of ecosystem stability following exposure. All other

2052 16
0 217217
5 218218
2062 219219
0 220220
6 221221
2072
0 222222
7 223223
224224
225225
226226
227227
228228
229229
230230
231231
232232
233233
234234
235235
236236
2082
0
8
2092
0
9
2102
1
0
2112
1
1
2122
1
2
2132
1
3
2142
1
4
2152
1
5
2162

m
on
it
or
in
g
an
d
sa
m
pl
in
g
pr
oc
ed
ur
es
de
sc
ri
be
d
be
lo
w
w
er
e
co
nd
uc
te
d
us
in
g
th
e
no
n-
ra
di
oa
cti
ve
,
su
rr

ogate aquatic mesocosms.

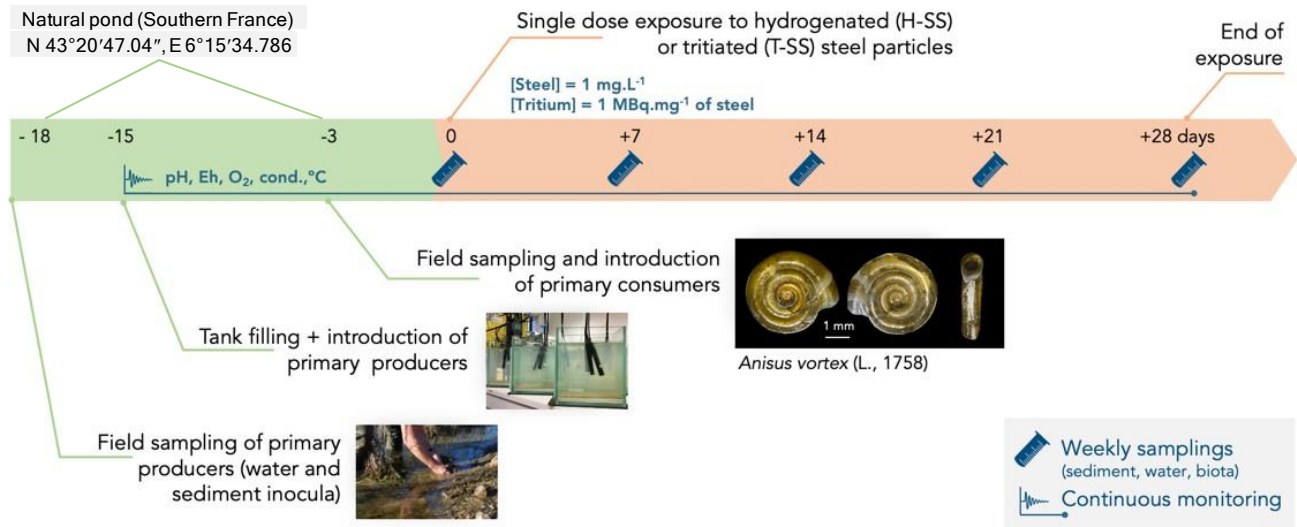


Figure 2. Schematic of the set-up, sampling, and monitoring of the freshwater indoor mesocosm experiments performed in the Tritium lab in CEA Saclay (France) and the CEREGE mesocosm facilities (France).

2.4 Aquatic mesocosm monitoring

For each mesocosm, multiparameter probes (Odeon® Open X) were installed (~20 cm below the air-water interface and 7 cm above the sediment) to monitor the temperature ($^{\circ}\text{C} \pm 0.5$ $^{\circ}\text{C}$), pH (unit ± 0.1 unit), redox potential ($\text{mV} \pm 1$ mV), electrical conductivity ($\mu\text{S}/\text{cm} \pm 2$ $\mu\text{S}/\text{cm}$), and dissolved O_2 ($\text{mg}\cdot\text{L}^{-1} \pm 0.1$ $\text{mg}\cdot\text{L}^{-1}$) in the water column for the entire duration of the experiment. The number of colloidal particles suspended in the water column was monitored weekly at 10 cm below the water surface using an optical particle counter (Flowcell FC200S + HR, Occhio®, Belgium). Particles with sizes ranging from 0.2 to 52 μm in the water column were considered.

2.5 Organism viability and behavior

Picobenthos and picoplankton (cells between 0.2 to 2 μm) concentrations were determined at the surface of the sediment (0.5 ± 0.1 mm depth) and in the water column (10 cm below the air-water interface) on a weekly basis. To determine picoplankton concentrations, water (10 mL) and sediment (15 mL) were sampled at days 0 and 28, treated with formaldehyde (3.7%), and stored at 4°C until counting. Counting was performed by mixing 10 μL of each sample with 5 μL 3 μM SYTO® 9 Green Fluorescent Nucleic Acid Stain on a glass slide and observing the number of cells in five different zones using a fluorescence microscope. The concentration of picoplankton ($\text{cells}\cdot\text{mL}^{-1}$) was reported as the mean \pm standard deviation of the five different zones. The benthic grazing snail, *A. vortex*, was observed weekly for viability and localization within the mesocosm (i.e., at the water surface or in the sediment) as an indication of potential behavioral changes. These behavioral changes are considered as a short time response and are both ecologically relevant and sensitive to environmental stressors.^{38,39}

238 2.6 Tritium and SS particle quantification in different environmental compartments of lentic 239 ecosystem

240 The tritium and the SS particle distributions in the mesocosms were quantified by respectively
241 measuring the tritium and main stainless steel metals (i.e., Fe, Cr, Ni, Mo, Mn), in the surficial
242 sediments, water column, and the *A. vortex* organisms. Sampling was performed weekly over 4
243 weeks (i.e. Days 0, 7, 14, 21 and 28). The surficial sediments were sampled at three different
244 locations and then pooled before drying 24 h at 50 °C. The estimated depth sampled using this
245 procedure was 0.32 ± 0.07 cm below the water /sediment interface. The water column (10 mL) was
246 sampled with a pipette at 10 cm below the surface of the water. The soluble fraction of the water
247 column was also collected for tritium and metal analysis by sampling aliquots of surface water (4
248 mL) at the same depth and centrifuging them in Amicon® Ultra-4 3 KDa centrifugal filter devices
249 (3000 MWCO, size retention limit ~ 1 nm, Merck-Millipore®) at 4000xg for 1 h to separate the
250 soluble and particulate fractions. Concerning the benthic organisms, ten *A. vortex* were sampled at
251 weeks 2 and 4, rinsed with clean Volvic® water (3 mL), and stored after drying 24 h at 50 °C.

252 Concerning the radioactivity (i.e., tritium) measurements, liquid scintillation counting was performed
253 using a Tri-Carb 2910TR analyzer from Perkin Elmer. Two types of measurements were performed,
254 either a direct measurement in the case of water samples, or after acid digestion in the case of the
255 solid samples (i.e., surficial sediments and *A. vortex*). The solid samples were analyzed after drying
256 (24 h at 50 °C), grinding, and acid digestion (3 volumes of 37% HCl Normatom® and 1 volume of
257 65% HNO₃ Normatom® for 48 h). The resulting solution contained a high concentration of ions and
258 the particle digestion induced a coloration of the solution. The digestion solution was therefore
259 diluted with 3 volumes of ultrapure water before measurement to limit quenching effects during
260 liquid scintillation counting.

261 Before ICP-MS elemental analysis for metal content, the water column and *A. vortex* rinse samples
262 (2 mL) were acid-digested at ambient temperature (3 mL 37% HCl Normatom® + 1 mL 65% HNO₃
263 Normatom®) for 48 h. Sediment and *A. vortex* samples were first ground using a mortar and pestle,
264 then mineralized at 180 °C by using a microwave digestion system (ultraWAVE, Milestone, Italy)
265 prior to ICP-MS analysis. For elemental analysis of sediment samples (50 mg), a mixture of 3 acids
266 (1.5 mL HCl 37% (Normatom®), 1 mL HNO₃ 65%, 1 mL of HF 47%-51%) was used, while *A.*
267 *vortex* organisms (50 mg) were digested in 1 mL HCl 37%, 1 mL HNO₃ 65%, 1 mL H₂O₂ 30%-32%
268 (PlasmaPure®) and 0.5 mL HF 47%-51%. All digested residues were diluted to 10 mL with ultrapure
269 water before analysis of Fe, Cr, Ni, Mo, and Mn concentrations using a PerkinElmer NexION 300X
270 quadrupole ICP-MS.

271 Although the main elements (i.e., Fe, Cr, Ni, Mo, Mn) comprising the SS particles were quantified in
272 each environmental compartment (i.e., water column, surficial sediment, and primary consumers),
273 not all elements could be used as tracers due to high background concentrations (Experimental S2
274 and Figure S4). Three elements (i.e., Cr, Ni, and Mo) were found to be suitable as tracers of the SS
275 particles (Figures S1). For clarity, only the data associated with using Mo as a tracer of SS in water
276 and sediment is presented, however comparable results which support the same conclusions were
277 obtained using Cr and Ni as tracers (Figures S5 & S7).

278

279

280

281

282

283 3 Results and Discussion

284 3.1 Tritiated stainless steel particle fate, behavior, and impacts in the planktonic 285 compartment

286 3.1.1 Tritium and SS behavior and fate in the water column

287 Figures 3A & 3B show the Mo concentrations (tracer of SS particles) measured in the water column
288 as a function of time. No significant increase in either the total Mo concentration ($\sim 0.6\text{-}0.7\ \mu\text{g}\cdot\text{L}^{-1}$) or
289 the dissolved Mo concentration ($\sim 0.5\text{-}0.6\ \mu\text{g}\cdot\text{L}^{-1}$) was observed in the water column of mesocosms
290 contaminated with H-SS during the one-month experiment. This highlights the fast kinetics of SS
291 particle removal from the water column that occurred during the first week. The lack of an increase
292 in Mo concentration in the dissolved fraction over the entire experiment duration is consistent with
293 the slow dissolution kinetics of SS. The negligible SS solubility was further confirmed by the lack of
294 other SS metals (i.e. Cr and Ni) being released into the dissolved phase (Figure S5).

295 Figure 3C gives the tritium activity in the water column following exposure to the T-SS. Seven days
296 after contamination significant tritium activity was measured in the water column, which remained
297 stable over time. The $\sim 150\ \text{Bq}\cdot\text{mL}^{-1}$ measured in the water column corresponded to $16 \pm 2\%$ of the
298 total tritium injected. To identify whether the tritium was bound to particles (SS or natural suspended
299 particles) or dissolved, ^3H activity was also measured after ultrafiltration of the water at 3 KDa. The
300 similar tritium activities measured before and after ultrafiltration allowed us to conclude that the
301 tritium measured in the water column of the mesocosms was fully dissolved (Figure 3D).

302 Understanding the distribution of tritium between the stainless steel surface, near surface, and bulk
303 metal is necessary for determining how the tritium is released from the T-SS particles in freshwater
304 ecosystems. Matsuyama et al.⁴⁰ suggested that the tritium atoms trapped by oxidized layers at the SS
305 surface easily react with water molecules and are quickly released in water at ambient temperature.
306 We evaluated the short-term release kinetics of ^3H release using a batch experiment and estimated
307 that $12 \pm 1.5\%$ of the total ^3H is released after 48 hours (Figure S6). Thereafter, the ^3H release did
308 not change significantly up to 92 hours ($14 \pm 1\%$ ^3H release) or even after 28 days ($16 \pm 2\%$) in the
309 mesocosms, which indicates that a quasi-equilibrium state had been reached.⁴¹

3103 318318
1 319319
0 320320
321321
322322
323323
324324
325325
326326

3113
1
1
3123
1
2
3133
1
3
3143
1
4
3153
1
5
3163
1
6
3173
1
7

A) Total Mo concentration ($\mu\text{g.L}^{-1}$) and (B) dissolved Mo concentration ($\mu\text{g.L}^{-1}$) in the water column of the control and H-SS exposed mesocosms. (C) Total ^3H activity (Bq.mL^{-1}) and (D) dissolved ^3H activity (Bq.mL^{-1}) in the water column of the H-SS and T-SS exposed mesocosms. Statistical differences between exposed and control mesocosms were evaluated with the Student's t- test; ** $p < 0.05$.

3.1.2 Homo-aggregation versus hetero-aggregation of tritiated steel particles

Two mechanisms can be involved in the fast removal of SS from the water column and their settling at the surface of the sediment: homo-aggregation between SS particles and/or hetero-aggregation with natural colloids. Indeed, natural colloids present in the mesocosm water (e.g. suspended clays, natural organic matter) can cause the formation and settling down of hetero-aggregates.²⁷ In the mesocosm water, the number of colloids in the 0.2-1 μm fraction (mostly kaolinite clay) was close to 10^5 particles. mL^{-1} (Figure 1). No significant differences in the number of colloids were observed after steel particle injection, indicating that hetero-aggregation was not predominant under these experimental conditions.

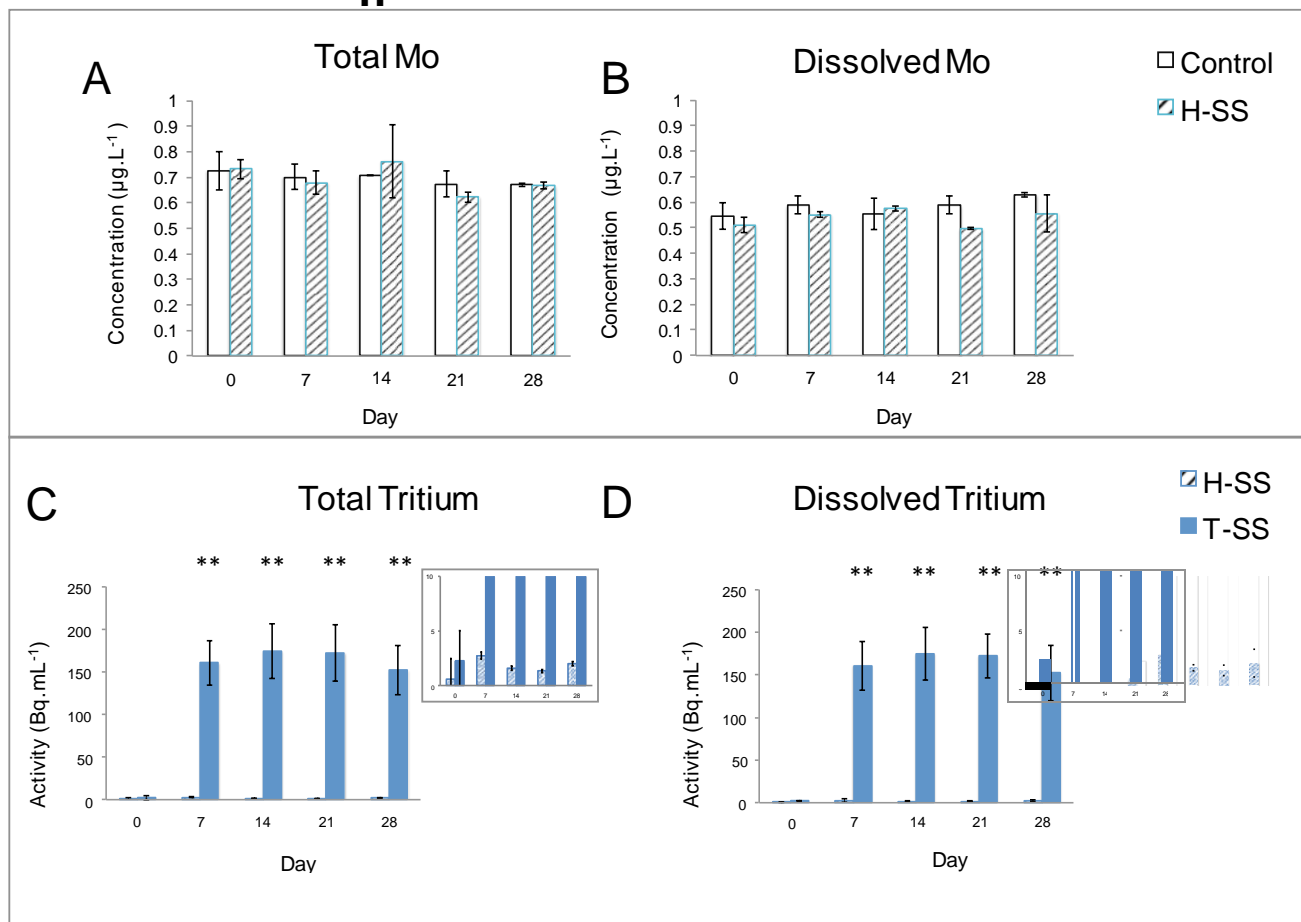
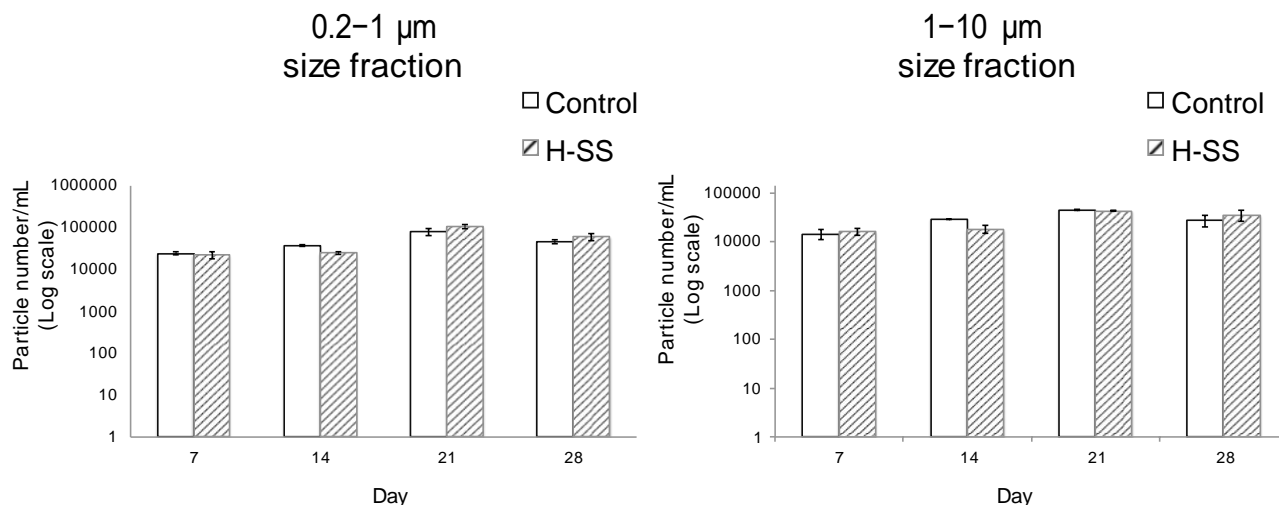


Figure 3.

3273
2
7



3283
2 **Figure 4.** Number of suspended materials (0.2-1 µm and 1-10 µm) in uncontaminated water from
8 control mesocosms and mesocosms contaminated with steel particles. X-axis: days.

3293
2 Moreover, because of the pH and ionic strength of the mesocosm water column, SS particles are
9 colloiddally unstable and will likely homo-aggregate (Ref 22, 23). Using Stokes' law the particle
3303 sedimentation velocity can be calculated:⁴²

$$v = \frac{2(\rho_p - \rho_f)gR^2}{9\mu}$$

3313
3
1
3323
3
2
3333
3
3
3343
3
4
3353
3
5
336 where v is the velocity ($\text{m}\cdot\text{s}^{-1}$), g the gravitational field strength ($\text{m}\cdot\text{s}^{-2}$), R the radius of the spherical
337 particle (m), ρ_p the mass density of the particle ($\text{kg}\cdot\text{m}^{-3}$), ρ_f the mass density of the fluid ($\text{kg}\cdot\text{m}^{-3}$), and
338 μ the viscosity ($\text{kg}\cdot\text{m}^{-1}\cdot\text{s}^{-1}$). With this equation, the $\sim 3\ \mu\text{m}$ SS particle population is expected to settle
339 within about 35 minutes, while the $\sim 0.8\ \mu\text{m}$ particle population would be expected to settle within
340 about 500 minutes (8 hours). The undetectable change in the number of natural colloids in the water
341 column (i.e. no decrease over time) associated with the fast kinetics of SS particle sedimentation, led
342 to the conclusion that homo-aggregation and gravitational settling in the most favorable mechanism
343 of steel particle partitioning in the mesocosms.

345 3.1.3 Favorable bio-physical-chemical conditions in the planktonic compartment

346 During the contamination phase, several physical-chemical and microbial parameters were monitored

347 to assess the global response of the mesocosms to the presence of the SS particles in the planktonic
348 compartment. The monitored physical-chemical parameters were constant over the contamination
349 period and close to the those measured on the field the day of sampling (with the exception of the
350 temperature): dissolved O₂ (80–93 %, 7–9 mg.L⁻¹), redox potential (414 ± 72 mV), conductivity (300
351 ± 4 μS.cm⁻¹), temperature (15.8 ± 0.8 °C), and pH (7.6 ± 0.2) (Figure S2). The number of
352 picoplankton (cells between 0.2 and 2 μm) measured in the water column at days 0 and 28 remained
353 constant over time, i.e. between 10⁴ and 10⁵ cells.mL⁻¹ (Figure S3). Moreover, no significant
354 differences were observed between control and contaminated mesocosms, thus no picoplankton
355 mortality resulted from the SS particle exposure.

356 On the whole, the ecological conditions of the mesocosm water column remained favorable during
357 the exposure to H-SS and T-SS with oxygenation, pH, temperature, redox potential, conductivity, and
358 the number of primary producers all in the range of natural conditions. This is consistent with the
359 selected exposure scenario and the low concentrations measured in the water column, which has been
360 found to be acutely non-toxic for the ecosystem mimicked.^{43–46}

362 3.2 Tritiated stainless steel particle accumulation and impacts in the benthic compartment

363 3.2.1 Tritium and SS behavior and fate in the surficial sediment

364 Given the relatively low particle stability in the water column, as well as the likelihood of the homo-
365 aggregation scenario discussed above, a significant accumulation in the surficial sediments was
366 expected. In Figures 5A & 5B, the Mo concentrations determined in the surficial sediment and in its
367 interstitial water were plotted. Despite the large variability attributed to sampling heterogeneity,
368 significant differences in the Mo concentrations measured in the sediment were observed compared
369 to the control at each sampling time. Concentrations averaging between 19 ± 6 mg Mo.kg⁻¹ sediment
370 (day 7) and 10 ± 2 mg Mo.kg⁻¹ sediment (day 14, 21, and 28) were measured. Given these
371 concentrations, we estimated that at the end of the experiment, 132 ± 37 % of the total SS had settled
372 down in the surficial sediment. Similar Mo concentrations (~ 0.6 µg.L⁻¹) in the sediment interstitial
373 water (Figure 5B) compared to the water column (Figures 3A & 3B) indicated that the interstitial
374 water was in equilibrium with the water column. Similar results were also obtained for Cr and Ni
375 concentrations, further confirming the settling down of the SS particles in the surficial sediment
376 (Figure S7).

377
378 Regarding the tritium concentration in the benthic compartment, Figure 5C highlights that the ³H
379 activity in surficial sediment reached 267 ± 57 Bq.mg⁻¹ of sediment after 28 days. The ³H activity in
380 the interstitial water of the surficial sediment (Figure 5D) was also measured and the results (~ 170
381 Bq.mL⁻¹) obtained at each sampling time again confirmed that the interstitial water was in
382 equilibrium with the water column (Figure 3D). Two hypotheses can be supported by these results: i)
383 the tritium found in the sediment is still bound to the SS particles, ii) the tritium in the sediment has
384 been first released from the SS particles and then adsorbed at the surface of inorganic or organic
385 phases of the sediment. Assuming that after 28 days in the surficial sediment, all the ³H (267 ± 57
386 Bq.mg⁻¹ of sediment) is still bound to the SS (9.6 ± 1.2 mg Mo.kg⁻¹ of sediment), this leads to an
387 estimated particle activity of 0.64 ± 0.14 MBq.mg⁻¹ of SS. Taking into consideration the ³H lost to
388 the water column ($\sim 16\%$), this value does not fully represent the expected activity of 0.84 ± 0.2
389 MBq.mg⁻¹ for the SS particles, likely due to the sampling and measurement heterogeneities, but still
390 accounts for an $\sim 80\%$ recovery of ³H and suggests that the first hypothesis is the most favored. All
391 these results highlight that the surficial sediments concentrate the pollution and will be an important
392 sink of incidental tritiated (nano)particles potentially released during nuclear power plant
393 dismantling.

394394

395395

3963 404404
9 405405
6 406406
407407
408408
409409
410410
411411
412412
413413
414414
415415
416416
417417
418418

3973
9
7
3983
9
8
3993
9
9
4004
0
0
4014
0
1
4024
0
2
4034
0
3

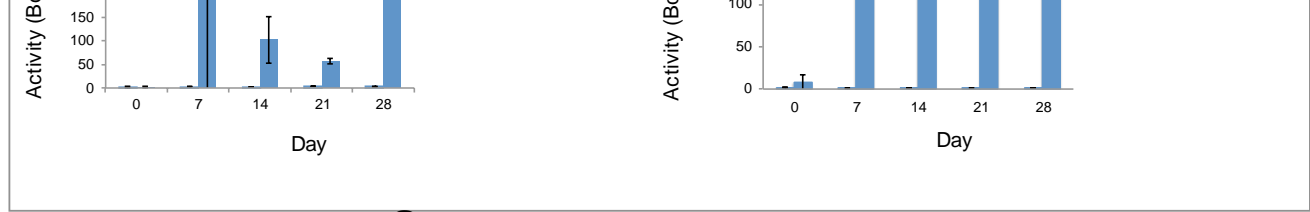
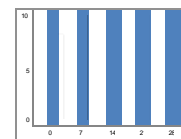


Figure 5. (A) Mo concentration (mg.kg^{-1}) in surficial sediments and (B) in the interstitial water ($\mu\text{g.L}^{-1}$) of the control and H-SS exposed mesocosms and (C) ^3H activity (Bq.mg^{-1}) in surficial sediments and (D) in the interstitial water (Bq.mL^{-1}) of the H-SS and T-SS exposed mesocosms. Statistical differences between exposed and control mesocosms were evaluated with the Student's t-test; ** $p < 0.05$.

3.2.2 Tritiated stainless steel particle uptake and impacts on freshwater organisms

A. vortex are benthic grazers that eat algae and biofilms at the sediment/water interface. Since the tritiated steel particles are concentrated in the sediment, these benthic grazers live and feed in a sensitive ecological niche. The active (ingestion) and passive (adsorption of the shell) uptake of SS particles and ^3H was determined by analyzing the elemental content of *A. vortex* before and after rinsing at 14 and 28 days.

Using Mo as the SS tracer, a passive interaction (e.g., adsorption on the shell) between the particles and the snails was observed with ~ 0.8 ng of Mo per snail ($\sim 0.005\%$ of injected SS particles) measured in the rinse water at day 28. Moreover, a significant Mo concentration ($0.22 \pm 0.06 \text{ mg.kg}^{-1}$) and ^3H activity ($4.25 \pm 1.36 \text{ Bq.mg}^{-1}$) were measured in the rinsed snails at day 14, suggesting an active uptake (Figures 4A and 4B). These concentrations at day 14 correspond to $<0.01\%$ of the SS and $<0.01\%$ of the ^3H initially injected after subtraction of the background of the relevant controls. Assuming that all the ^3H taken up is still bound to the SS, this leads to a particle activity of $0.51 \pm$



4194
1
9
4204
2
0
4214
2
1
4224
2
2 429429
4234 430430
2 431431
3 432432
4244 433433
2 434434
4
4254
2
5
4264
2
6
4274
2
7
4284
2
8

0.
40
M
B
q.
m
g⁻¹
of
S
S.
A
s
fo
r
th
e
se
di
m
en
t,
th
is
va
lu
e
do
es
no
t
fu
ll
y
re
pre
sen
t
th
e
ex
pe
ct
ed
S
S
pa
r
ti

cle activity of $0.84 \pm 0.2 \text{ MBq.mg}^{-1}$ after the initial 16% ^3H release in the water column, likely due in this case to a low $[\text{Mo}]$ as well as sampling and measurement heterogeneities, but still supports the hypothesis that the ^3H taken up remained bound to the SS particles. After 28 days, the concentrations and activity ($[\text{Mo}] = 0.16 \pm 0.03 \text{ mg.kg}^{-1}$, $[\text{Ni}] = 0.86 \pm 0.15 \text{ mg.kg}^{-1}$, $[\text{Cr}] = 0.65 \pm 0.23 \text{ mg.kg}^{-1}$, ^3H activity of 4.65 Bq.mg^{-1}) remained constant. Although the measurement of ^3H at day 28 only represents the result from one mesocosm due to loss of the replicate sample, this value is consistent with the ^3H amount estimated to be found in the snails using Mo as the tracer for the SS particles and assuming that the tritium remains particle-bound.

A. vortex

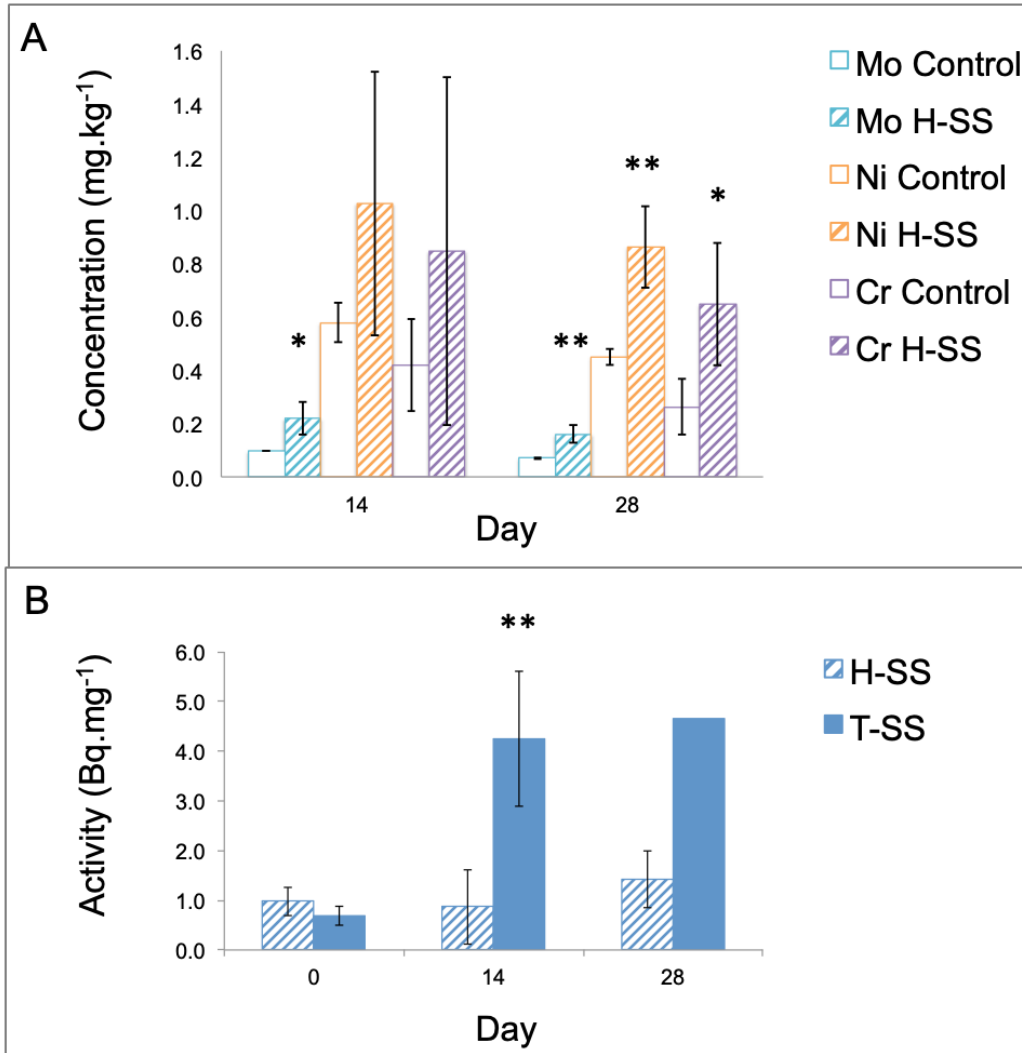
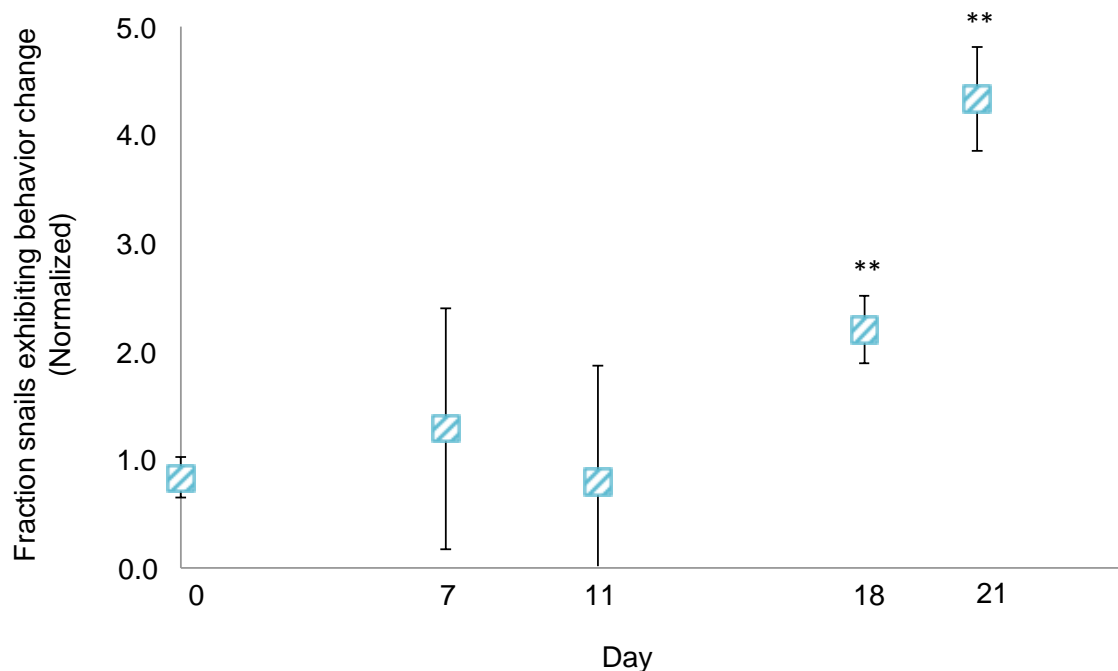


Figure 6. Concentration of A) metals (mg/kg) and B) ^3H activity (Bq/mg) accumulated in *A. vortex*. Statistical differences between exposed and control mesocosms were evaluated with the Student's t-test; * $p < 0.1$, ** $p < 0.05$.

435 Following exposure to H-SS in the surficial sediment, no acute toxicity was observed towards *A.*
436 *vortex* (<1% of mortality) nor the primary producers (no change in the number of picobenthos $\sim 10^6$
437 cells.mL⁻¹) over the duration of the experiment (Figure S3).
438 Nevertheless, aquatic organisms can respond to stress with a combination of physiological adaptation
439 and behavioral responses.⁴⁷ Behavioral modification in animals is one of the most sensitive indicators
440 of environmental stress.⁴⁸ Herein, we noticed that *A. vortex* behavior was affected following exposure
441 to the H-SS particles. After 18 and 21 days of exposure, there was a significant increase in the
442 fraction of snails burrowing at the sediment surface, with fractions of 2.2 ± 0.3 and 4.3 ± 0.5 ,
443 respectively after normalization to controls (Figure 7). Of note, a fraction of 1.0 indicates no
444 behavioral change with respect to control organisms. Such negative effects on living traits of
445 freshwater snails have already been observed following a decrease in temperature,⁴⁹ exposure to
446 metals⁵⁰ or pesticides,⁵¹ and also in the presence of invasive predator populations.⁵² These behavioral
447 changes could have implications on the ecology, population dynamics and habitat features of a
448 species.⁵³ Being less mobile in/at the surface of the sediment, the snails will be more exposed to
449 predators, the interactions between snails will be reduced, and the grazing patterns of snails will be
450 affected, which will impact their feeding regimen, the periphyton communities, and thus the overall
451 balance and health of the freshwater ecosystem.⁵⁴
452 Based on the feeding regimen of the snails and on previous mesocosm experiments performed with
453 TiO₂, CuO and CeO₂ engineered nanoparticles, it is likely that the SS (nano)particles are localized in
454 the digestive gland of *A. vortex* where they undergo enzymatic digestion^{43-45,55}. In depth
455 characterization of the localization (at tissular and cellular scale) and speciation of the metals (e.g.,
456 Fe, Ni, Cr, Mo) is required to better understand the biodistribution and biotransformation of the SS
457 particles, as well as the bio-physico-chemical mechanisms of toxicity. For instance, the delay of 11 to
458 18 days before observing significant changes (Figure 7) could be attributed to the more or less rapid
459 modification (depending on the group of invertebrates) of the enzymatic systems which regulate
460 behavior (carboxylesterases, glutathione S-transferase, cholinesterase, etc.). These toxicokinetic
461 effects on the sensitivity have already been observed in the case of pesticides.⁵⁶⁻⁶⁰ and would require
462 confirmation for H-SS exposure. Moreover, a thorough characterization of the biological responses in
463 the presence of T-SS is still required. Indeed, with mixtures (as in tritiated stainless steel
464 (nano)particles), we could observe additive effects (e.g., the sum of ³H and metal toxicities),
465 synergistic effects (inducing toxic effects greater than the sum of the effects of the individual
466 chemicals) or also antagonistic effects (where the combined effect of is less toxic than the individual
467 effects).^{61,62} The potential combined radiotoxicity (due to ³H) and particle toxicity (due to SS
468 particles) needs to be further understood.
469
470
471



472
 473 **Figure 7.** Fraction of snail population residing at/in sediment surface in H-SS contaminated
 474 mesocosms normalized to controls. Statistical differences between exposed and control mesocosms
 475 were evaluated with the Student's t-test; ** $p < 0.05$.
 476

477 **Conclusions**

478
 479 The present indoor freshwater mesocosm experiment permitted the analysis of the environmental fate
 480 and impact of anthropogenic tritiated stainless steel (nano)particles and dissolved tritium following a
 481 one-time contamination scenario. Our results demonstrated that upon entering the aquatic
 482 environment, the stainless steel (nano)particles exhibited no significant solubility, rapidly settled
 483 down, and accumulated at the water/sediment interface. During the exposure, ~16% of the tritium
 484 was rapidly lost to the water column, while the majority of the tritium (>80 %) remained associated
 485 to the stainless steel (nano)particles or sediment. Thus, tritium association with or transport by
 486 incidental anthropogenic (nano)particles generated during dismantling activities will drive its
 487 environmental behavior and fate. The accumulation of stainless steel particles and the associated
 488 tritium in the sediment represents a high exposure of the benthic ecological niche. While no acute
 489 toxicity was observed towards the picoplanktonic and picobenthic communities or the benthic
 490 grazers, the benthic grazers presented significant behavioral changes in the presence of stainless steel
 491 particles, exhibiting increased burrowing at the sediment surface despite low steel uptake (<0.01 %).
 492 This behavior change is an indicator of environmental stress and further studies are thus warranted to
 493 understand the mechanisms related to this response, evaluate any combined radiotoxicity and particle
 494 toxicity, and confirm if benthic grazer gastropods such as *A. vortex* can be used as indicator species
 495 for this type of radioactive particle contamination. Altogether, these results provide some of the first
 496 elements of knowledge on the potential dosimetry and environmental impacts of tritiated stainless
 497 steel particles, which will allow for improved hazard and risk management.

498

499

500 **Declaration of Competing Interest**

501 The authors declare that they have no known competing financial interests or personal relationships
502 that could have influenced the work reported in this paper.

503 **CRedit Author Contribution Statement**

504 **Danielle L. Slomberg:** Conceptualization, Data curation, Formal analysis, Investigation,
505 Methodology, Project Administration, Writing – original draft. **Mélanie Auffan:** Conceptualization,
506 Data curation, Formal analysis, Investigation, Methodology, Project Administration, Supervision,
507 Writing – original draft. **Mickaël Payet:** Data curation, Investigation, Methodology, Writing –
508 review & editing. **Andrea Carboni:** Methodology, Investigation. **Amazigh Ouaksel:** Investigation.
509 **Lenka Brousset:** Investigation. **Bernard Angeletti:** Investigation. **Christian Grisolia:** Funding
510 acquisition, Project administration. **Alain Thiéry:** Investigation, Writing – review & editing. **Jérôme**
511 **Rose:** Conceptualization, Funding acquisition, Project Administration, Supervision, Writing – review
512 & editing.

513 **Funding**

514 This project has received funding from the Euratom Research and Innovation Programme 2014–2018
515 under grant agreement no. 754586. The views and opinions expressed herein do not necessarily
516 reflect those of the European Commission.

517 **Acknowledgments**

518 We thank the CNRS for funding the IRP INOVE. The authors thank the Molecular Labeling and Bio-
519 organic Chemistry (SCBM) unit at CEA Paris-Saclay, and in particular Sébastien Garcia-Argote and
520 Cristelle Bisson, for hosting the tritium experiments. We also thank Andrea Campos of Aix-Marseille
521 University/Fédération Sciences Chimiques Marseille (FSCM) for SEM-EDS imaging and analysis.

522 **Data Availability Statement**

523 The datasets for this study can be found in the MESOCOSM database platform
524 [<https://mesocosmdb.cerege.fr/>], as well as the repository Zenodo
525 [<https://zenodo.org/record/7255814>, DOI: 10.5281/zenodo.7255814].

526 **References**

- 527
- 528 [1] McCarthy, J.; Zachara, J., ES&T Features: Subsurface transport of contaminants, *Env. Sci.*
529 *Technol.* 23 (1989) 496-502. <https://doi.org/10.1021/es00063a602>.
- 530
- 531 [2] Penrose, W. R.; Polzer, W. L.; Essington, E. H.; Nelson, D. M.; Orlandini, K. A., Mobility of
532 plutonium and americium through a shallow aquifer in a semiarid region, *Env. Sci. Technol.* 24
533 (1990) 228-234. <https://doi.org/10.1021/es00072a012>.
- 534
- 535 [3] Orlandini, K. A.; Penrose, W. R.; Harvey, B. R.; Lovett, M. B.; Findlay, M. W., Colloidal
536 behavior of actinides in an oligotrophic lake, *Env. Sci. Technol.* 24 (1990) 706-712.
537 <https://doi.org/10.1021/es00075a015>.
- 538
- 539 [4] Wigginton, N. S.; Haus, K. L.; Hochella Jr, M. F., Aquatic environmental nanoparticles, *J.*
540 *Environ. Monit.* 9 (2007) 1306–1316. <https://doi.org/10.1039/B712709J>.
- 541
- 542 [5] Hochella Jr, M. F.; Lower, S. K.; Maurice, P. A.; Penn, R. L.; Sahai, N.; Sparks, D. L.;
543 Twining, B. S., Nanominerals, mineral nanoparticles, and earth systems, *Science* 319 (2008) 1631–

544 1635. <https://doi.org/10.1126/science.1141134>.
545
546 [6] Westerhoff, P.; Atkinson, A.; Fortner, J.; Wong, M. S.; Zimmerman, J.; Gardea-Torresdey, J.;
547 Ranville, J.; Herckes, P., Low risk posed by engineered and incidental nanoparticles in drinking
548 water, *Nat. Nanotechnol.* 13 (2018) 661–669. <https://doi.org/10.1038/s41565-018-0217-9>.
549
550 [7] Makhraj, V. A.; Garkusha, I. E.; Aksenov, N. N.; Chuvilo, A. A.; Chebotarev, V. V.;
551 Landman, I.; Malykhin, S. V.; Pestchanyi, S.; Pugachov, A. T., Dust generation mechanisms under
552 powerful plasma impacts to the tungsten surfaces in ITER ELM simulation experiments, *J. Nucl.*
553 *Mater.* 438 (2013) S233–S236. <https://doi.org/10.1016/j.jnucmat.2013.01.034>.
554
555 [8] Acsente, T.; Negrea, R. F.; Nistor, L. C.; Logofatu, C.; Matei, E.; Birjega, R.; Grisolia, C.;
556 Dinescu, G., Synthesis of flower-like tungsten nanoparticles by magnetron sputtering combined with
557 gas aggregation, *Eur. Phys. J. D* 69 (2015) 1-7. <https://doi.org/10.1140/epjd/e2015-60097-4>.
558
559 [9] Liger, K.; Grisolia, C.; Cristescu, I.; Moreno, C.; Malard, V.; Coombs, D.; Markelj, S.,
560 Overview of the TRANSAT (TRANSversal Actions for Tritium) project. *Fusion Eng. Des.* 136
561 (2018) 168–172. <https://doi.org/10.1016/j.fusengdes.2018.01.037>.
562
563 [10] Sobrido, M.S.; Bernard, E.; Angeletti, B.; Malard, V.; George, I.; Chaurand, P.; Uboldi, C.;
564 Orsière, T.; Dine, S.; Vrel, D.; and Rousseau, B., Oxidative transformation of Tungsten (W)
565 nanoparticles potentially released in aqueous and biological media in case of Tokamak (nuclear
566 fusion) Lost of Vacuum Accident (LOVA), *Comptes Rendus. Géoscience*, 352 (2020) 539-558.
567 <https://doi.org/10.5802/crgeos.41>.
568
569 [11] Decanis, C.; Kresina, M.; Canas, D., Methodology to identify appropriate options to manage
570 tritiated waste, *Fusion Eng. Des.* 136 (2018) 276–281.
571 <https://doi.org/10.1016/j.fusengdes.2018.02.008>.
572
573 [12] Boyer, C.; Vichot, L.; Fromm, M.; Losset, Y.; Tatin-Froux, F.; Guétat, P.; Badot, P. M.,
574 Tritium in plants: A review of current knowledge, *Environ. Exp. Bot.* 67 (2009) 34–51.
575 <https://doi.org/10.1016/j.envexpbot.2009.06.008>.
576
577 [13] Kudryasheva, N. S.; Rozhko, T. V., Effect of low-dose ionizing radiation on luminous marine
578 bacteria: Radiation hormesis and toxicity, *J. Environ. Radioact.* 142, (2015) 68–77.
579 <https://doi.org/10.1016/j.jenvrad.2015.01.012>.
580
581 [14] Nie, B.; Fang, S.; Jiang, M.; Wang, L.; Ni, M.; Zheng, J.; Yang, Z.; Li, F., Anthropogenic
582 tritium: Inventory, discharge, environmental behavior and health effects, *Renew. Sustain. Energy*
583 *Rev.* 135, (2021) 110188. <https://doi.org/10.1016/j.rser.2020.110188>.
584
585 [15] Bondareva, L.; Kudryasheva, N.; Tananaev, I., Tritium: Doses and responses of aquatic living
586 organisms (model experiments), *Environments* 9 (2022) 51.
587 <https://doi.org/10.3390/environments9040051>.
588
589 [16] Kim, S. B.; Baglan, N.; Davis, P. A., Current understanding of organically bound tritium
590 (OBT) in the environment, *J. Environ. Radioact.* 126 (2013) 83–91.
591 <https://doi.org/10.1016/j.jenvrad.2013.07.011>.
592

- 593 [17] Kim, S. B.; Shultz, C.; Stuart, M.; McNamara, E.; Festarini, A.; Bureau, D. P., Organically
594 bound tritium (OBT) formation in rainbow trout (*Oncorhynchus Mykiss*): HTO and OBT-spiked food
595 exposure experiments, *Appl. Radiat. Isot.* 72 (2013) 114–122.
596 <https://doi.org/10.1016/j.apradiso.2012.10.001>.
597
- 598 [18] Kim, S. B.; Bredlaw, M.; Rousselle, H.; Stuart, M., Distribution of organically bound tritium
599 (OBT) activity concentrations in aquatic biota from Eastern Canada, *J. Environ. Radioact.* 208 (2019)
600 105997. <https://doi.org/10.1016/j.jenvrad.2019.105997>.
601
- 602 [19] Jaeschke, B. C.; Bradshaw, C., Bioaccumulation of tritiated water in phytoplankton and
603 trophic transfer of organically bound tritium to the blue mussel, *Mytilus Edulis*, *J. Environ. Radioact.*
604 115, (2013) 28–33. <https://doi.org/10.1016/j.jenvrad.2012.07.008>.
605
- 606 [20] Jacobs, D. G., Sources of tritium and its behavior upon release to the environment, AEC
607 Critical Review Series (1968). <https://doi.org/10.2172/4799828>.
608
- 609 [21] Puls, R. W.; Powell, R. M., Transport of inorganic colloids through natural aquifer material:
610 implications for contaminant transport, *Env. Sci. Technol.* 26 (1992) 614–621.
611 <https://doi.org/10.1021/es00027a027>.
612
- 613 [22] Tran, E.; Zavrin, M.; Kersting, A. B.; Klein-BenDavid, O.; Teutsch, N.; Weisbrod, N.,
614 Colloid-facilitated transport of ²³⁸Pu, ²³³U and ¹³⁷Cs through fractured chalk: Laboratory
615 experiments, modelling, and implications for nuclear waste disposal, *Sci. Total Environ.* 757 (2021)
616 143818. <https://doi.org/10.1016/j.scitotenv.2020.143818>.
617
- 618 [23] Midander, K.; Pan, J.; Leygraf, C., Elaboration of a test method for the study of metal release
619 from stainless steel particles in artificial biological media, *Corros. Sci.* 48 (2006) 2855–2866.
620 <https://doi.org/10.1016/j.corsci.2005.10.005>.
621
- 622 [24] Song, Y. Y.; Bhadeshia, H. K. D. H.; Suh, D.-W., Stability of stainless-steel nanoparticle and
623 water mixtures, *Powder Technol.* 272 (2015) 34–44. <https://doi.org/10.1016/j.powtec.2014.11.026>.
624
- 625 [25] Gutierrez, M. F.; Ale, A.; Andrade, V.; Bacchetta, C.; Rossi, A.; Cazenave, J., Metallic, metal
626 oxide, and metalloid nanoparticles toxic effects on freshwater microcrustaceans: An update and basis
627 for the use of new test species, *Water Environment Research* 93 (2021) 2505–2526.
628 <https://doi.org/10.1002/wer.1637>.
629
- 630 [26] Wang, T. and Liu, W., Emerging investigator series: metal nanoparticles in freshwater:
631 transformation, bioavailability and effects on invertebrates, *Environ. Sci.: Nano*, 9 (2022) 2237–2263.
632 <https://doi.org/10.1039/D2EN00052K>.
633
- 634 [27] Auffan, M.; Flahaut, E.; Thill, A.; Mouchet, F.; Carriere, M.; Gauthier, L.; Achouak, W.;
635 Rose, J.; Wiesner, M.R.; Bottero, J. Y., Ecotoxicology: Nanoparticle reactivity and living organisms.
636 In *Nanoethics and nanotoxicology* (2011) 325–357. Berlin, Heidelberg: Springer Berlin Heidelberg.
637
- 638
- 639 [28] Vernon, E. L.; Jha, A. N.; Ferreira, M. F.; Slomberg, D. L.; Malard, V.; Grisolia, C.; Payet,
640 M.; Turner, A., Bioaccumulation, release and genotoxicity of stainless steel particles in marine
641 bivalve molluscs, *Chemosphere* 303 (2022) 134914.

642 <https://doi.org/10.1016/j.chemosphere.2022.134914>.
643

644 [29] Praetorius, A.; Labille, J.; Scheringer, M.; Thill, A.; Hungerbühler, K.; Bottero, J.-Y.,
645 Heteroaggregation of titanium dioxide nanoparticles with model natural colloids under
646 environmentally relevant conditions, *Environ. Sci. Technol.* 48 (2014) 10690–10698.
647 <https://doi.org/10.1021/es501655v>.
648

649 [30] Slomberg, D. L.; Ollivier, P.; Radakovitch, O.; Baran, N.; Sani-Kast, N.; Miche, H.;
650 Borschneck, D.; Grauby, O.; Bruchet, A.; Scheringer, M.; Labille, J., Characterisation of suspended
651 particulate matter in the Rhone River: Insights into analogue selection, *Environ. Chem.* 13 (2016)
652 804–815. <https://doi.org/10.1071/EN15065>.
653

654 [31] Slomberg, D. L.; Ollivier, P.; Miche, H.; Angeletti, B.; Bruchet, A.; Philibert, M.; Brant, J.;
655 Labille, J., Nanoparticle stability in lake water shaped by natural organic matter properties and
656 presence of particulate matter, *Sci. Total Environ.* 656 (2019) 338–346.
657 <https://doi.org/10.1016/j.scitotenv.2018.11.279>.
658

659 [32] Joo, S. H.; Zhao, D., Environmental dynamics of metal oxide nanoparticles in heterogeneous
660 systems: A review, *J. Hazard. Mater.* 322 (2017) 29–47.
661 <https://doi.org/10.1016/j.jhazmat.2016.02.068>.
662

663 [33] Bour, A.; Mouchet, F.; Silvestre, J.; Gauthier, L.; Pinelli, E., Environmentally relevant
664 approaches to assess nanoparticles ecotoxicity: A review, *J. Hazard. Mater.* 283 (2015) 764–777.
665 <https://doi.org/10.1016/j.jhazmat.2014.10.021>.
666

667 [34] Carboni, A.; Slomberg, D. L.; Nassar, M.; Santaella, C.; Masion, A.; Rose, J.; Auffan, M.,
668 Aquatic mesocosm strategies for the environmental fate and risk assessment of engineered
669 nanomaterials, *Environ. Sci. Technol.* 55 (2021) 16270–16282.
670 <https://doi.org/10.1021/acs.est.1c02221>.
671

672 [35] Auffan, M.; Tella, M.; Santaella, C.; Brousset, L.; Paillès, C.; Barakat, M.; Espinasse, B.;
673 Artells, E.; Issartel, J.; Masion, A.; Rose, J.; Wiesner, M. R.; Achouak, W.; Thiéry, A.; Bottero, J.-Y.,
674 An adaptable mesocosm platform for performing integrated assessments of nanomaterial risk in
675 complex environmental systems, *Sci. Rep.* 4 (2014) 5608. <https://doi.org/10.1038/srep05608>.
676

677 [36] Gensdarmes, F.; Payet, M.; Malard, V.; Grisolia, C., Report on production of steel particles,
678 TRANSAT Deliverable 3.1, Horizon 2020 Programme, (2019). [https://transat-h2020.eu/wp-](https://transat-h2020.eu/wp-content/uploads/2020/04/TRANSAT-D3.1-Report-on-Production-of-Steel-Particles.pdf)
679 [content/uploads/2020/04/TRANSAT-D3.1-Report-on-Production-of-Steel-Particles.pdf](https://transat-h2020.eu/wp-content/uploads/2020/04/TRANSAT-D3.1-Report-on-Production-of-Steel-Particles.pdf)
680

681 [37] Payet, M.; Report on tritiation of cement and steel particles, TRANSAT Deliverable 3.3,
682 Horizon 2020 Programme, (2020). [https://transat-h2020.eu/wp-content/uploads/2020/04/TRANSAT-](https://transat-h2020.eu/wp-content/uploads/2020/04/TRANSAT-D3.3-Report-on-tritiation-of-cement-and-steel-particles.pdf)
683 [D3.3-Report-on-tritiation-of-cement-and-steel-particles.pdf](https://transat-h2020.eu/wp-content/uploads/2020/04/TRANSAT-D3.3-Report-on-tritiation-of-cement-and-steel-particles.pdf)
684

685 [38] Sanchez, W.; Porcher, J.-M., Fish biomarkers for environmental monitoring within the water
686 framework directive of the European Union, *TrAC Trends Anal. Chem.* 28 (2009) 150–158.
687 <https://doi.org/10.1016/j.trac.2008.10.012>.
688

689 [39] Shinn, C., Impact of toxicants on stream fish biological traits, Doctoral dissertation -
690 Université de Toulouse, Université Toulouse III-Paul Sabatier, 2010.

691
692 [40] Matsuyama, M.; Chen, Z.; Nisimura, K.; Akamaru, S.; Torikai, Y.; Hatano, Y.; Ashikawa, N.;
693 Oya, Y.; Okuno, K.; Hino, T., Trapping and depth profile of tritium in surface layers of metallic
694 materials, *J. Nucl. Mater.* 417 (2011) 900–903. <https://doi.org/10.1016/j.jnucmat.2011.04.005>.
695
696 [41] Sharpe, M.; Fagan, C.; Shmayda, W. T., Distribution of tritium in the near surface of type 316
697 stainless steel. *Fusion Sci. Technol.*, 75 (2019) 1053–1057.
698 <https://doi.org/10.1080/15361055.2019.1644136>.
699
700 [42] Lamb, H. (1932) *Hydrodynamics* (6th ed.). Cambridge University Press.
701
702 [43] Tella, M.; Auffan, M.; Brousset, L.; Morel, E.; Proux, O.; Chanéac, C.; Angeletti, B.; Pailles,
703 C.; Artells, E.; Santaella, C.; Rose, J.; Thiéry, A.; Bottero, J.-Y., Chronic dosing of a simulated pond
704 ecosystem in indoor aquatic mesocosms: Fate and transport of CeO₂ nanoparticles, *Environ. Sci.*
705 *Nano* 2 (2015) 653–663. <https://doi.org/10.1039/C5EN00092K>.
706
707 [44] Tella, M.; Auffan, M.; Brousset, L.; B.; Issartel, J.; Kieffer, I.; Pailles, C.; Morel, E.;
708 Santaella, C.; Angeletti, B.; Artells, E.; Rose, J.; Thiéry, A.; Bottero, J.-Y., Transfer, transformation,
709 and impacts of ceria nanomaterials in aquatic mesocosms simulating a pond ecosystem, *Environ. Sci.*
710 *Technol.* 48 (2014) 9004–9013. <https://doi.org/10.1021/es501641b>.
711
712 [45] Châtel, A.; Auffan, M.; Perrein-Ettajani, H.; Brousset, L.; Métais, I.; Chaurand, P.; Mouloud,
713 M.; Clavaguera, S.; Gandolfo, Y.; Bruneau, M.; Masion, A.; Thiéry, A.; Rose, J.; Mouneyrac, C.,
714 The necessity of investigating a freshwater-marine continuum using a mesocosm approach in
715 nanosafety: The case study of TiO₂ MNM-based photocatalytic cement, *NanoImpact* 20 (2020)
716 100254. <https://doi.org/10.1016/j.impact.2020.100254>.
717
718 [46] Auffan, M.; Santaella, C.; Brousset, L.; Tella, M.; Morel, E.; Ortet, P.; Barakat, M.; Chaneac,
719 C.; Issartel, J.; Angeletti, B.; Levard, C.; Hazemann, J.-L.; Wiesner, M.; Rose, J.; Thiéry, A.; Bottero,
720 J.-Y., The shape and speciation of Ag nanoparticles drive their impacts on organisms in a lotic
721 ecosystem, *Environ. Sci. Nano* 7 (2020) 3167–3177. <https://doi.org/10.1039/DOEN00442A>.
722
723 [47] MacInnes, J. R.; Thurberg, F. P., Effects of metals on the behaviour and oxygen consumption
724 of the mud snail. *Mar. Pollut. Bull.* 4 (1973) 185–186. [https://doi.org/10.1016/0025-326X\(73\)90225-](https://doi.org/10.1016/0025-326X(73)90225-7)
725 7.
726
727 [48] Eisler, R.; Carney, G. C.; Lockwood, A. P. M.; Perkins, E. J.; Cole, H. A., Behavioural
728 responses of marine poikilotherms to pollutants. *Philos. Trans. R. Soc. Lond. B Biol. Sci.* 286 (1997)
729 507–521. <https://doi.org/10.1098/rstb.1979.0043>.
730
731 [49] Buerger, H., Movement and burrowing of *Helisoma Trivolvis* (Say) (Gastropoda,
732 Planorbidae) in a Small Pond, *Can. J. Zool.* 53 (1975) 456–464. <https://doi.org/10.1139/z75-059>.
733
734 [50] Kamble, S. B.; Kamble, N. A., Behavioural changes in freshwater snail *Bellamya Bengalensis*
735 due to acute toxicity of copper sulphate and *Acacia Sinuata*, *Int. J. Sci. Environ. Technol.* 3 (2014)
736 1090-1104.
737
738 [51] Elias, D.; Bernot, M. J., Effects of individual and combined pesticide commercial
739 formulations exposure to egestion and movement of common freshwater snails, *Physa Acuta* and

- 740 *Helisoma Anceps*, Am. Midl. Nat. 178 (2017) 97–111. <https://doi.org/10.1674/0003-0031-178.1.97>.
741
- 742 [52] Levri, E. P.; Berkheimer, C.; Wilson, K.; Xu, J.; Woods, T.; Hutchinson, S.; Yoder, K.;
743 Zhang, X.; Li, X., The cost of predator avoidance behaviors in an invasive freshwater snail, Freshw.
744 Sci. 39 (2020) 476–484. <https://doi.org/10.1086/710107>.
745
- 746 [53] Lillebø, A. I.; Pardal, M. Â.; Marques, J. C., Population structure, dynamics and production
747 of *Hydrobia Ulvae* (Pennant) (Mollusca: Prosobranchia) along an eutrophication gradient in the
748 Mondego Estuary (Portugal), Acta Oecologica 20 (1999) 289–304. [https://doi.org/10.1016/S1146-](https://doi.org/10.1016/S1146-609X(99)00137-X)
749 609X(99)00137-X.
750
- 751 [54] Burris, J. A.; Bamford, M. S.; Stewart, A. J., Behavioral responses of marked snails as
752 indicators of water quality, *Environ. Toxicol. Chem.* 9 (1990) 69–76.
753 <https://doi.org/10.1002/etc.5620090109>.
754
- 755 [55] Auffan, M.; Liu, W.; Brousset, L.; Scifo, L.; Pariat, A.; Sanles, M.; Chaurand, P.; Angeletti,
756 B.; Thiery, A.; Masion, A.; Rose, J. Environmental Exposure of a Simulated Pond Ecosystem to CuO
757 Nanoparticle Based-Wood Stain throughout Its Life Cycle. *Environ. Sci. Nano* 2018, 5, 2579–2589.
758 <https://doi.org/10.1039/C7EN00494J>.
759
- 760 [56] Martínez Morcillo, S.; Yela, J. L.; Capowiez, Y.; Mazzia, C.; Rault, M.; Sanchez-Hernandez,
761 J. C., Avoidance behaviour response and esterase inhibition in the earthworm, *Lumbricus Terrestris*,
762 after exposure to chlorpyrifos, *Ecotoxicology* 22 (2013) 597–607. [https://doi.org/10.1007/s10646-](https://doi.org/10.1007/s10646-013-1051-3)
763 013-1051-3.
764
- 765 [57] Otero, S.; Kristoff, G., *In vitro* and *in vivo* studies of cholinesterases and carboxylesterases in
766 *Planorbarius Corneus* exposed to a phosphorodithioate insecticide: Finding the most sensitive
767 combination of enzymes, substrates, tissues and recovery capacity, *Aquat. Toxicol.* 180 (2016) 186–
768 195. <https://doi.org/10.1016/j.aquatox.2016.10.002>.
769
- 770 [58] Jouni, F.; Sanchez-Hernandez, J. C.; Mazzia, C.; Jobin, M.; Capowiez, Y.; Rault, M.,
771 Interspecific differences in biochemical and behavioral biomarkers in endogeic earthworms exposed
772 to ethyl-parathion, *Chemosphere* 202 (2018) 85–93.
773 <https://doi.org/10.1016/j.chemosphere.2018.03.060>.
774
- 775 [59] Jouni, F.; Sanchez-Hernandez, J. C.; Brouchoud, C.; Capowiez, Y.; Rault, M., Role of soil
776 texture and earthworm casts on the restoration of soil enzyme activities after exposure to an
777 organophosphorus insecticide, *Appl. Soil Ecol.* 187 (2023) 104840.
778 <https://doi.org/10.1016/j.apsoil.2023.104840>.
779
- 780 [60] Sedeño-Díaz, J. E.; López-López, E., Oxidative stress in *Physella Acuta*: An integrative
781 response of exposure to water from two rivers of Atlantic Mexican Slope, *Front. Physiol.* 13 (2022)
782 1805. <https://doi.org/10.3389/fphys.2022.932537>.
783
- 784 [61] Roell, K. R.; Reif, D. M.; Motsinger-Reif, A. A., An introduction to terminology and
785 methodology of chemical synergy—Perspectives from across disciplines, *Front. Pharmacol.* 8 (2017)
786 158. <https://doi.org/10.3389/fphar.2017.00158>.
787
- 788 [62] Li, M.; Liu, W.; Slaveykova, V. I., Effects of mixtures of engineered nanoparticles and

789 metallic pollutants on aquatic organisms, *Environments* 7 (2020) 27.
790 <https://doi.org/10.3390/environments7040027>.